Journal of Fluorescence, Vol. 7, No. 4, 1997

Fluorescence and Rotational Dynamics of Dityrosine

Greg S. Harms,[1] Steve W. Pauls,[1] John F. Hedstrom,[2] and Carey K. Johnson[1,3]

Received August 22, 1997; revised December 3, 1997; accepted December 29, 1997

We have examined the lifetimes and rotational correlation times of dityrosine emission by time-correlated single-photon counting. We first noticed dityrosine fluorescence in samples of tyrosine and tyrosine dipeptides by its characteristic red-shifted emission at 400 to 430 nm. The longer rotational correlation time relative to tyrosine proved that this fluorescence emanated from a distinct species. Comparison with the fluorescence properties of synthesized dityrosine established the identity of the emitting species. Fluorescence intensity decays of dityrosine are generally characterized by two decay components, one with a lifetime in the range of 150 to 800 ps and another between 2.5 and 4.5 ns. We found no evidence for an excited-state reaction, since a rising phase (negative-amplitude component) was not observed. In the pH range from 4 to 10, two ground-state species exist in equilibrium with $pK_a \approx 7$. Both species exhibit two fluorescence decays. The average fluorescence lifetime increases gradually with pH over the pH range from 4 to 10 and decreases at pH 2. Anisotropy decays were measured for dityrosine and the alanine–dityrosine–alanine and leucine–dityrosine–leucine dipeptides. The rotational correlation times of dityrosine and dityrosine dipeptides increase linearly with van der Waals volumes. The slope indicates a stronger solute–solvent interaction than predicted with "stick" boundary conditions. It is suggested that these interactions result from the presence of two zwitterionic pairs.

KEY WORDS: Dityrosine; tyrosine; dipeptides; fluorescence intensity; time-correlated single-photon counting; fluorescence anisotropy; rotational correlation times.

INTRODUCTION

In the course of our investigation of the fluorescence properties of tyrosine (see the preceding paper,[1] we noticed emission at wavelengths of around 400 nm. The fluorescence and anisotropy decays that characterized the emission at this wavelength could not be attributed to tyrosine itself. Further investigation led us to identify this component as a tyrosine dimer, *o,o*-dityrosine, consisting of two tyrosine residues connected by an ortho linkage between the phenolic groups of tyrosine (see Fig. 1).[2]

Dityrosine fluorescence may be a useful marker of oxidative conditions in biological systems. Since dityrosine forms *in vivo*, it may also serve as a useful intrinsic fluorescent probe of protein environments and internal motions. For example, orientational motions of dityrosine can be monitored in membrane protein environments. The presence of dityrosine has been tied to cross-linking in biological materials.[3–10] Reports suggest that dityrosine forms in highly oxidative environments[2,11–21] via a free radical mechanism.[15] The production of dityrosine has been associated with a number of factors, including free radicals,[17,18,22] UV irradiation,[2,12,15] age-related accumulation of fluorescent lipofusion pigments,[16] tobacco smoke,[23] and cataractous

[1] Department of Chemistry, University of Kansas, Lawrence, Kansas 66045.

[2] Department of Chemistry, Luther College, Decorah, Iowa 52101.

[3] To whom correspondence should be addressed. e-mail: cjohnson@eureka.chem.ukans.edu. Fax: 785-864-5396.

1053-0509/97/1200-0283$12.50/0

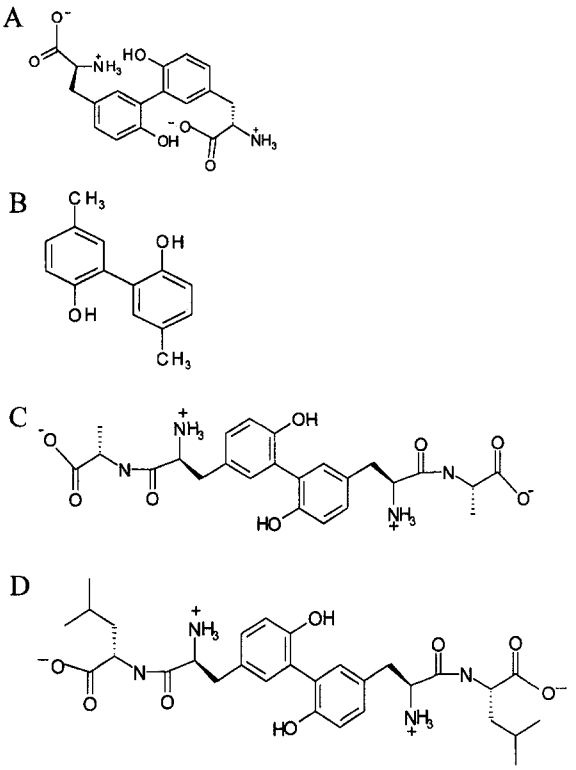

Fig. 1. Structures of dityrosine (A), bicresol (B), and the dityrosine dipeptides alanine–dityrosine–alanine (C) and leucine–dityrosine–leucine (D).

human lens proteins.[24,25] Thus, the characteristic fluorescence of dityrosine may be diagnostic of processes associated with aging or oxidative damage in physiological systems.

The absorption and fluorescence spectra of dityrosine closely resemble the corresponding spectra of *o,o'*-bicresol.[2] Dityrosine has also been characterized by NMR,[5,14] IR,[6] HPLC,[6,21,26,27] absorption,[2,28] and fluorescence spectroscopy.[2,28] Time resolution of the 400-nm emission adds a new dimension to determination of dityrosine fluorescence and may facilitate its detection without the necessity for peptide degradation of samples. The experimentally determined average fluorescence lifetimes of dityrosine range from 2.5 to 9 ns.[29-31] Dityrosine fluorescence decay was apparently first observed as a 400-nm emission of histone H1 under certain conditions, with a 9-ns lifetime whose origin was undetermined.[32] Small and Anderson later reported a single-exponential decay of 4.30 ns for a pure dityrosine sample at pH 7.0 in 5.0 m*M* MOPS buffer.[29] More recently, Kungl *et al.*[30,33] reported multiple-exponential decays including a rising component and proposed an excited-state reaction involving deprotonation of a phenol group and torsion of the biphenolic bond.

In this paper, we report fluorescence lifetimes, rotational times, and quantum yields for dityrosine and dityrosine-containing peptides and proteins. The rotational diffusion and reorientational dynamics of dityrosine itself and of peptides and proteins containing dityrosine are examined in different environments. Our results differ in several respects from those in Ref. 30. We observed multiple fluorescence decays components but found no evidence for an excited-state reaction. Analysis of the rotational dynamics indicated a stronger interaction of dityrosine and cross-linked dityrosine peptides with aqueous solvent than in the corresponding tyrosine and tyrosine peptides.

MATERIALS AND METHODS

Chemicals and Preparations

L-Tyrosine, tyrosine–alanine, tyrosine–leucine, and *p*-cresol were purchased from Sigma and were checked by HPLC for purity. Dityrosine and dityrosine dipeptides were prepared by the method of Amadò *et al.*[15] and were purified by gradient HPLC of 0 to 20% acetonitrile and 0.01% TFA for a span of 60 min at a flow rate of 8 ml/min with 300-nm absorbance detection. Bicresol was prepared and purified by the method of Westerfield and Lowe[11] and purified by HPLC of 0 to 100% acetonitrile and 0.01% TFA over 60 min with 300-nm absorbance detection. Samples were subsequently concentrated by rotary evaporation and analyzed by absorption, emission, and mass spectroscopy. The identity of the prepared sample was verified by comparing its spectroscopic properties, both continuous and time resolved, with those of a sample of dityrosine that was graciously provided by Dr. Stephen Fry and Dr. Geoffery Brady (Department of Botany, University of Edinburgh). All samples were dissolved in Nanopure water adjusted for pH or in 10 m*M* phosphate buffer prepared from Nanopure water. Sample concentrations of dityrosine, dityrosine dipeptides, and bicresol were kept at about 70 to 100 μ*M*. All solutions were bubbled with argon for at least 10 min with a slow gas flow to deoxygenate them prior to use.

Experimental Setup

The time-correlated single-photon counting (TCSPC) system, data collection, and data fitting procedures are described in detail in the preceding paper.[1]

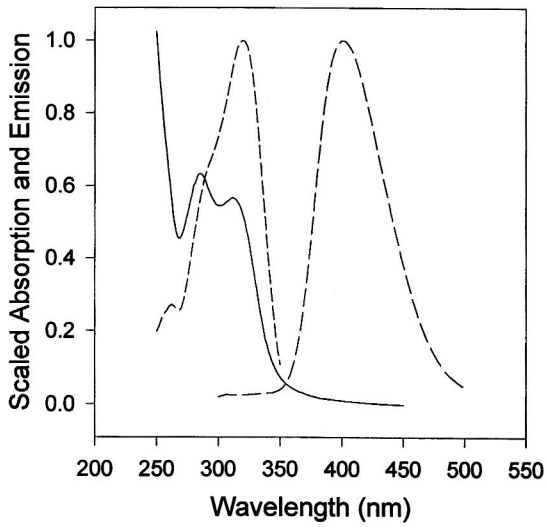

Fig. 2. Steady-state spectra of dityrosine. The solid line shows the absorption spectrum; the dashed lines show the excitation and emission spectra. The two peaks observed in the absorption spectrum correspond to two ground-state species, one protonated and one deprotonated (see text).

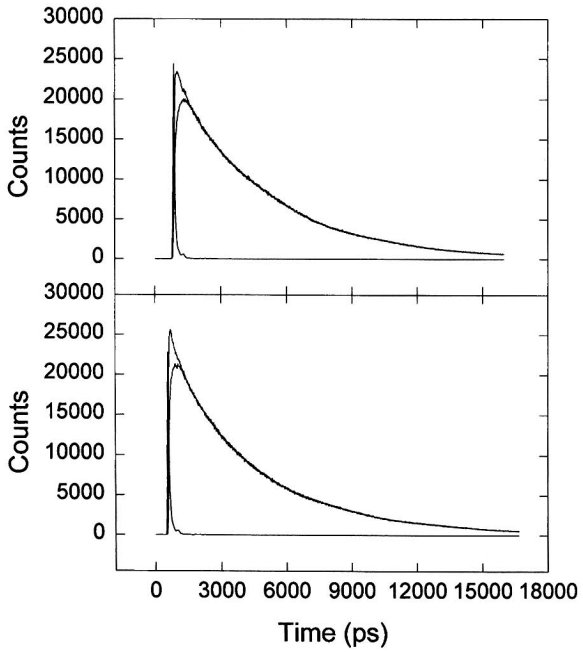

Fig. 3. Comparison of the fluorescence decays associated with emission at 400 nm in a synthesized dityrosine sample (top) and in a nominal tyrosine sample (5 m*M*; bottom). Excitation was at 287 nm. In each panel, the upper curve (solid line) shows the decay of fluorescence with polarization parallel to the excitation polarization, and the lower curve (dashed line) shows the decay of fluorescence with perpendicular polarization. The instrument function is also shown (short dashes). Fluorescence intensity and anisotropy decay parameters are given in Table I.

RESULTS AND DISCUSSION

Dityrosine and Dityrosine Dipeptide Fluorescence Decays

Figure 2 shows the steady-state absorption, excitation, and emission spectra of dityrosine at pH 7. Two peaks appear in the absorption spectrum, one at 285 nm and another at 315 nm. These peaks are associated with the protonated and deprotonated forms of dityrosine.[2,3,28,30,34,35] In contrast, the fluorescence spectrum is dominated by a single band with a maximum at ~400 nm. This emission band serves as a marker for dityrosine.

We first observed dityrosine emission in solutions of 5 m*M* tyrosine as purchased from Sigma. The results shown in Fig. 3 demonstrate first that solutions of 5 m*M* tyrosine have a distinct fluorescence lifetime and rotational time at an emission wavelength of 400 nm when photoexcited at 287 nm. The emission at 400 nm is characterized by a decay time that is much longer than that of tyrosine and tyrosine dipeptides (see Ref. 1). Furthermore, the rotational correlation time is more than triple that of tyrosine (see Table III). A literature search suggested that the 400-nm emission originated from dityrosine, which was evidently either contained in the tyrosine samples or formed over the course of the measurement.

To demonstrate the origin of the 400-nm emission, dityrosine was synthesized as described under Materials and Methods. The emission decays of the synthesized dityrosine were found to match closely the 400-nm emission from the tyrosine sample (see Fig. 3). A similar comparison with a dityrosine sample received from Dr. Stephen Fry and Dr. Geoffery Brady further verified the origin of the 400-nm emission. The essentially identical fluorescence decays and rotational times are strong evidence that the decays observed with the tyrosine and dipeptide solutions at 400-nm emission originate from dityrosine.

Dityrosine emission was also observed in dipeptide samples. The results are shown in Figs. 4 and 5. A summary of the fitting parameters for dityrosine and dityrosine dipeptides is given in Tables I and II. In each case, the 400-nm emission from a nominal tyrosine sample matched the decay characteristics of synthesized dityrosine within statistical error. We conclude that dityrosine exists as a component of samples of tyrosine and tyrosine-containing peptides. Although exposure of the sample to excitation light leads to additional buildup of dityrosine, the characteristic 400-nm emission seems to appear immediately when data collection begins. It

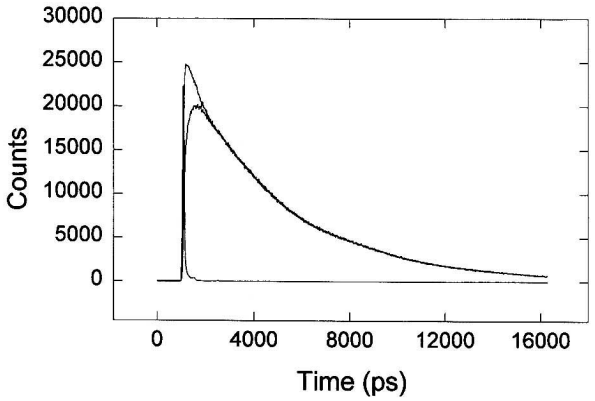

Fig. 4. Fluorescence decay of the alanine–dityrosine–alanine dipeptide at 400 nm with excitation at 287 nm. Decays are shown for fluorescence polarized parallel (top curve) and perpendicular (bottom curve) to the excitation polarization. Fluorescence intensity and anisotropy decay parameters are given in Table I.

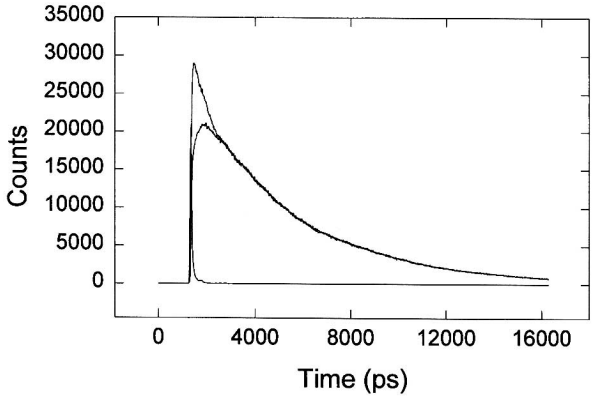

Fig. 5. Fluorescence decay of the leucine–dityrosine–leucine dipeptide at 400 nm with excitation at 287 nm. Decays are shown for fluorescence polarized parallel (top curve) and perpendicular (bottom curve) to the excitation polarization. Fluorescence intensity and anisotropy decay parameters are given in Table I.

Table I. Dityrosine Fluorescence Data

pH	λ_{ex} (nm)	λ_{em} (nm)	a_1	τ_1 (ns)	a_2	τ_2 (ns)	χ^2
2.0	300	400	0.23	0.791	0.77	2.754	1.7
4.0	300	400	0.21	0.374	0.79	3.967	2.1
6.0	300	400	0.15	0.344	0.85	4.126	2.0
7.0	300	400	0.11	0.216	0.89	4.326	1.4
8.0	300	400	0.09	0.160	0.91	4.406	2.2
10.0	300	400	0.08	0.154	0.92	4.490	1.9
2.0	288	400	0.24	0.940	0.76	2.399	1.6
4.0	288	400	0.20	0.970	0.80	4.180	1.9
6.0	288	400	0.18	2.120	0.82	4.210	1.9
7.0	288	400			1.00	4.222	1.8
8.0	288	400			1.00	4.421	2.0
10.0	288	400			1.00	4.458	2.1
7.0	288	350	0.97	0.057	0.002	4.257	
					0.001	0.655	1.1
7.0	300	380	0.58	0.093	0.42	4.360	2.7
7.0	300	430	0.21	0.270	0.79	4.430	2.5
8.0 (Borate buffer)	288	380	0.28 0.66	0.07 0.26	0.06	4.50	2.2

Table II. Dityrosine Dipeptide Fluorescence Data

Sample	λ_{ex}	λ_{em}	a_1	a_2	τ_1 (ns)	τ_2	r_0	τ_{rot} (ps)	χ^2
AdYA[a]	288	400	0.85	0.15	4.19	2.36	0.26	240	1.9
LdYL[b]	288	400	0.86	0.14	4.34	1.73	0.26	310	2.0

[a] Alanine–dityrosine–alanine.
[b] Leucine–dityrosine–leucine.

therefore seems likely that dityrosine exists as an impurity in preparations of tyrosine and peptides containing tyrosine.

We have recorded fluorescence decays of dityrosine at several emission wavelengths from 350 to 430 nm. The results are presented in Table I. The fluorescence decays over these wavelengths can be fit with two principal decay components: one in the range from 60 ps to about 1 ns and another of roughly 4.0 to 4.4 ns. The longer decay time prevails at longer wavelengths, whereas the strongly quenched decay at 350 nm is dominated by the shorter lifetime. Since we observe no evidence of an excited-state reaction, this emission appears to result from a heterogeneous ground-state population of dityrosine. A short decay time and blue-shifted emission is also observed for dityrosine complexed with borate.

Kungl *et al.*[30] have also reported fluorescence decays of dityrosine at several emission wavelengths. For $\lambda_{em} < 380$ nm, our results are in qualitative agreement with theirs (see Table I). However, at emission wavelengths of $\lambda > 380$ nm, Kungl *et al.* reported a rising phase of about 200 ps. They attributed this component to an excited-state process, such as an intramolecular torsional motion along the biphenolic bond. In contrast, we did not observe a negative-amplitude component (a rising phase) at any emission wavelength. The results that we present in this paper were obtained with an instrumental response function of less than 30-ps FWHM. In comparison, the instrumental response for fluorescence lifetime measurements in Ref. 30 was about 1.5-ns FWHM. This longer instrumental response time may

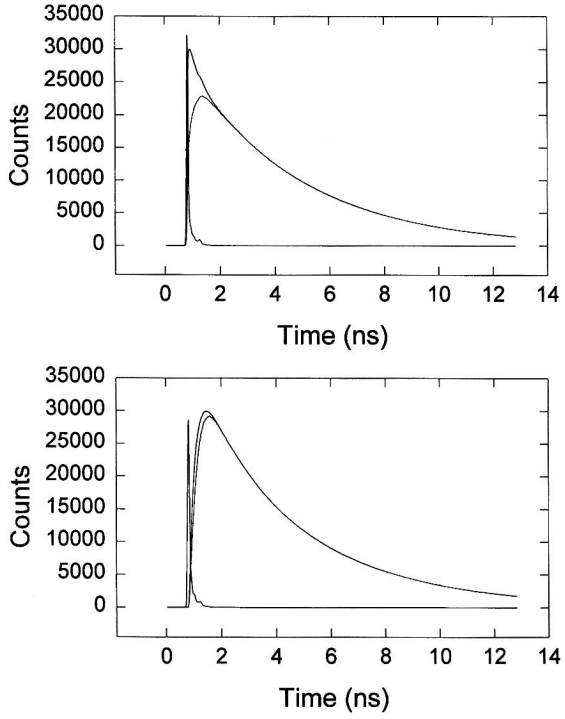

Fig. 6. Simulated fluorescence decay data for dityrosine with an actual instrument response function obtained from the TCSPC instrument. The sharp curve shows the instrument response function. Top: The parallel and perpendicular fluorescence decays simulated with the fitting parameters for dityrosine (see Table I) with two time constants, both with positive preexponential parameters. Bottom: The parallel and perpendicular fluorescence decays simulated with the fitting parameters reported in Ref. 45, consisting of a rise and decay phase. The simulated data should be compared to the actual experimental data in Fig. 3.

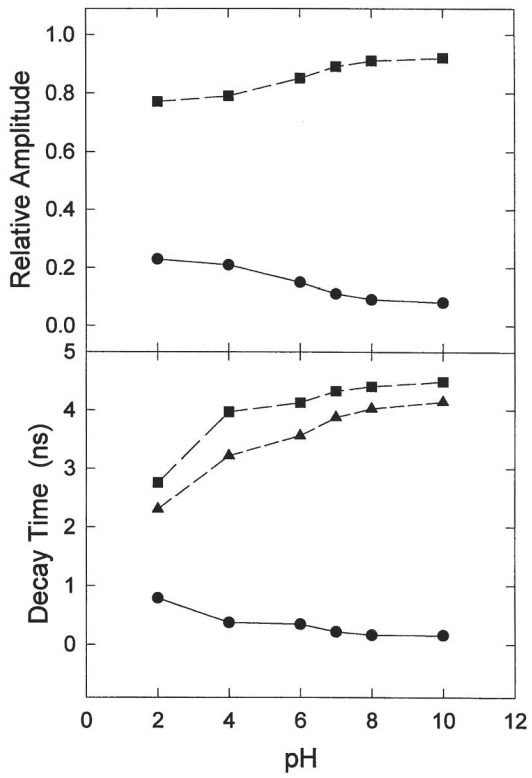

Fig. 7. pH dependence of the long (■) and short (●) components of the dityrosine emission. The amplitudes are shown in the top panel and the lifetimes in the bottom panel. The average lifetime (▲) is also shown in the bottom panel. Excitation wavelength, 300 nm for emission at 400 nm.

have resulted in uncertainties in the fitting parameters of subnanosecond process.

To test our ability to detect a subnanosecond rise time, simulated experimental decays were created by convoluting the instrument response function with a sum of exponential decays, following a method described by O'Connor and Phillips.[36] We tested both the actual instrumental response function used in this paper and also a 1.0-ns response function. Simulated data were generated with the decay parameters reported here and in Ref. 30 for both magic-angle and fluorescence depolarization scans. The simulated data were fit in the same way as actual TCSPC data. Figure 6 shows that for a subnanosecond component, the difference between a positive and a negative preexponential factor can be clearly distinguished. In contrast, given the same data, the 1.0-ns instrument response makes determination of the sign of the preexponential factor ambiguous in some cases. Given a positive preexponential factor for the subnanosecond decay convoluted with the 1.0-ns instrument response, two fits were found, one with a positive and one with a negative preexponential factor for the subnanosecond component. The positive has a slightly lower χ^2. In contrast, in data simulated with a 30-ps FWHM instrumental response, a positive amplitude is unambiguously recovered for the subnanosecond component decay component. We conclude that the fluorescence decay of dityrosine does not contain a significant subnanosecond rise component. Hence, there appears to be no evidence for an excited-state reaction leading to emission at $\lambda >$ 380 nm.

pH Dependence of Dityrosine Emission

Table I and Fig. 7 show the pH dependence of the fluorescence decay times of dityrosine from pH 2 to pH 10. Several observations can be made. First, the data are well represented by two decay times throughout this pH range. For emission at 300 nm, for example, one com-

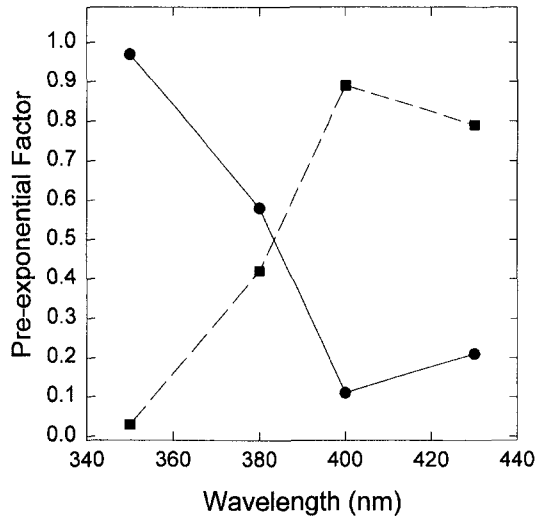

Fig. 8. Wavelength dependence of the long (■) and short (●) decay components in dityrosine emission. Excitation wavelengths, 288 nm for emission at 350 nm and 300 nm for emission at 380 to 450 nm.

ponent has lifetimes in the range of 150 to 800 ps, and the other has lifetimes between 2.7 and 4.5 ns. The amplitudes of these decay components are pH dependent, as shown in Fig. 7. We have also fit the decays to three exponentials. However, these fits resulted in a minor (<10%) long third component (6 to 8 ns) with only a modest improvement in the χ^2 values.

A second observation is that the fluorescence is quenched at low pH. A plot of the average lifetime as a function of pH, also shown in Fig. 7, illustrates the decreasing fluorescence yield at low pH values. This pH-dependent behavior can best be is described by titration of the carboxylate with a pK_a of about 2. The decrease in fluorescence lifetime at low pH values implies the formation of a dityrosine species with a protonated carboxylate group having a short fluorescence lifetime. Similar behavior has been observed for tyrosine.[1,37]

Another potential source of pH-dependent behavior is the phenol group, which has a pK_a of about 7[3,28,34,35] The pH dependencies of the absorption and fluorescence spectra of dityrosine have been reported previously. The absorption spectrum shifts from a peak at ca. 285 nm at a low pH, to about 316 nm at a high pH, with $pK_a \approx 7$.[2,3,28,30,34,35] Curiously, a distinct fluorescence peak corresponding to the protonated (pH <7) form of dityrosine was not observed.[2,28,30] This finding led Lehrer and Fasman to conclude that emission occurs from the deprotonated form, preceded by rapid excited-state proton transfer in the acidic form at pH values below about 7.[2] Fluorescence measurements showed a pH-dependent intensity of the fluorescence excited at 285 nm, suggesting an excited-state pK_a of about 2.[35]

This picture faces a challenge from the results presented in Table I, because a negative amplitude or rising phase has not been resolved in the present study. Excited-state proton transfer would be expected to manifest itself as a rise time in the emission of the anionic form following excitation of protonated dityrosine. Since this rise time is not observed, it is necessary to conclude that excited-state proton transfer, if it occurs at all, must occur on a shorter time scale than the resolution of the TCSPC instrument, that is, in less than ~10 ps. In this case, excited-state proton transfer leads rapidly to the anionic excited state, which then fluoresces with the two observed lifetimes. These lifetimes, τ_1 and τ_2, might correspond to two conformations of dityrosine, one of which is strongly quenched. It is not possible to attribute the fast lifetime τ_1 to an excited-state mechanism, because such a process would be observable as a rise time in the fluorescence of the excited-state photoproduct.

Another explanation is also consistent with our observations. In this picture, two fluorescing species are postulated, corresponding to protonated and anionic ground-state species. In this view, excited-state proton transfer does not occur. Rather, both the protonated and the anionic forms of dityrosine decay with two lifetimes, one of 150 to 400 ps and the other of 4.0 to 4.5 ns (see Table I). The contribution from the short-lifetime component is more pronounced in the protonated form than in the anionic form. A plot of the fast and slow decay times in Table I (with excitation at 300 nm) as a function of pH in Fig. 7 suggests that the protonated form (pH < 7) is characterized by lifetimes of 300 to 400 ps and ~4.0 ns, and the anionic form (pH > 7) is characterized by lifetimes of ~150 ps and 4.5 ns. This pH dependence lends support to this second explanation. These two components may correspond to two ground-state conformations of dityrosine. We note also that at the lowest pH studied, pH 2, the fluorescence properties change, with a lower average lifetime. This may be a result of protonation of the carboxylate, with a pK_a of about 2, as in tyrosine.

The wavelength dependence of the short component at pH 7 suggests, in addition, that the emission of the short-lifetime component of the protonated form is shifted to the blue with respect to the dominant emission band at 400 nm (see Fig. 8). The blue shift of the short-lifetime component shown in Fig. 8 led us to examine carefully the steady-state fluorescence spectra of dityrosine over the pH range from 2 to 10. With excitation at 280 nm, a weak blue-shifted band appears at 330 to 340 nm in the emission spectrum at pH 2. At higher pH

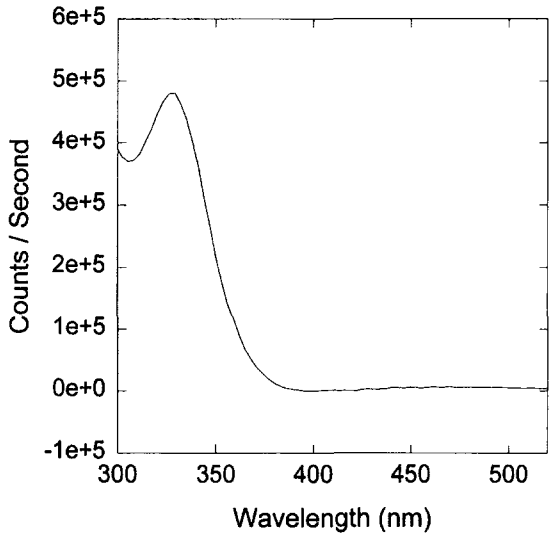

Fig. 9. Difference emission spectrum of dityrosine at pH 7. The 400-nm emission band was removed by subtracting the pH 10 emission spectrum.

Table III. Dityrosine Rotational Correlation Time Data

pH	λ_{ex} (nm)	λ_{em} (nm)	r_0	τ_{rot} (ps)	χ^2
2.0	288	400	0.26	180	1.6
4.0	288	400	0.26	170	2.2
6.0	288	400	0.26	156	2.2
7.0	288	400	0.26	146	1.8
8.0	288	400	0.26	136	1.5
10.0	288	400	0.26	130	1.4
7.0	300	380	0.26	125	2.7
7.0	300	400	0.26	150	1.7
7.0	300	430	0.26	130	2.5
8.0 (Borate buffer)	288	380	0.26	290	2.2

values, emission in the 300- to 350-nm region becomes very weak. However, Fig. 8 shows that this is the region associated with fast fluorescence components. We attribute this band to the fluorescence from the acidic form, with a lifetime of 300 to 400 ps. Subtraction of the main 400-nm fluorescence band (as measured at pH 10) from the fluorescence measured at pH 7 with excitation into the acidic form at 288 nm discloses the existence of a weak fluorescence band with a maximum at 330 nm (see Fig. 9). The subtracted spectrum in Fig. 9 confirms the presence of a second emission band, one that is very weak. The emission in the blue region is associated with the protonated (acidic) form, which absorbs in the region from 250 to 300 nm.

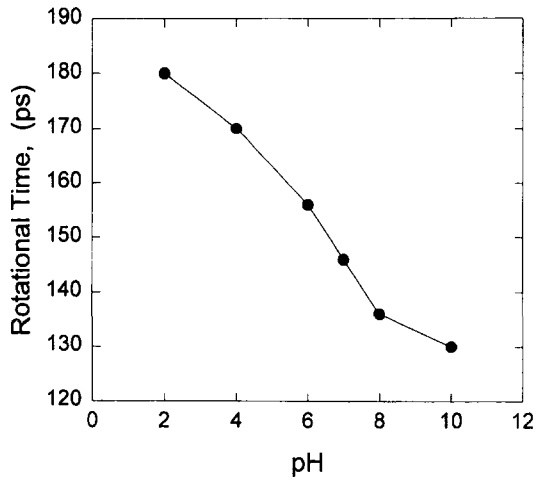

Fig. 10. pH dependence of the rotational correlation time of dityrosine. Excitation at 288 nm; emission at 400 nm.

The rotational time also decreases with increasing pH (see Table III and Fig. 10). This probably also results from the change of the protonation state, which alters the interaction of dityrosine with the aqueous solution. The ionized (acidic) form may experience a higher friction due to its net charge, leading to a longer rotational correlation time. A similar effect on the rotational correlation time of tyrosine was discussed in the preceding paper.[1] Another possibility, suggested by Mahmoud and Bialkowski,[28] is the formation of a dityrosine dimer. In this case, the decrease in rotational times with pH suggests that the dimers exist only when the phenolic hydrogens are present and that, as the pH increases, the dimers dissociate as the phenolic hydrogen is lost, possibly as a result of the formation of ionic charges.

Concentration and Solvent Dependence

The fluorescence and anisotropy decays of dityrosine as a function of concentration from 2 to 50 μM were also measured. Concentration changes in this range were found to have no effect on fluorescence or fluorescence anisotropy within statistical error. A previous study[28] suggested a concentration dependence of the emission intensity for concentrations above 15 μM. Since we do not observe any significant change in fluorescence lifetimes or rotational diffusion times with concentration at pH 7, we find no evidence for self-quenching or dimerization.

We also measured fluorescence spectra and fluorescence lifetimes for dityrosine in borate buffer (see Table I). The dityrosine–borate complex appears to open up

Table IV. Dityrosine Quantum Yields

Sample	pH	Conc.	Temp. (°C)	Quantum yield	τ_{rad} (ns)	Source
DT	4	~100 (μ*M*)	25	0.15	27	This work
DT	10	100	25	0.38	11	This work
BC	2	100	25	0.007	14	This work
BC	10	100	25	0.2	20	This work
DT	3.6	—	25	0.15	—	[2][a]
DT	10.7	—	25	0.22	—	[2]
BC	3.8	—	25	0.19	—	[2]
BC	10.8	—	25	0.24	—	[2]
DT	4	—	25	0.12	—	[37][a]
DT	10	—	25	0.16	—	[37]
DT	—	—	25	0.80	—	[34]

[a] Corrected relative to a quantum yield of 0.07 for tyrosine (see text).

two faster decay routes; the fluorescence decay fit contains three exponentials, of 0.07 ns (28%), 1.35 ns (66%), and 4.50 ns (6%).

Quantum Yield of Dityrosine

The quantum yield of dityrosine was determined for the acidic and basic forms at pH 4 and 10 by the method described in the preceding paper.[1] Radiative lifetimes of 27 and 11 ns were calculated from the absorption spectra at pH values of 4 and 10, respectively (see Table IV). The fluorescence quantum yields were then calculated from the measured fluorescence lifetimes. Results are shown in Table IV. We find values for the fluorescence quantum yield of 0.15 (pH 4) and 0.38 (pH 10). This result shows that the previously reported pH dependence of the quantum yield[38] is a consequence largely of the pH dependence of the radiative lifetime.

The fluorescence quantum yields reported here are somewhat lower than the fluorescence quantum yield reported by Lehrer and Fasman.[2] However, the fluorescent quantum yields in Ref. 2 were determined relative to a fluorescence yield of tyrosine that was assumed to have a value of 0.21.[39] If these values are calibrated instead to the quantum yield of tyrosine reported in the previous paper,[1] the adjusted values become 0.22 at pH 10.7 and 0.15 at pH 3.8. Similarly, Sakura and Fujimoto[38] reported fluorescence quantum yields for dityrosine relative to a reference quantum yield for tyrosine of 0.14.[40] When adjusted to a fluorescence quantum yield of 0.07 for tyrosine,[1] their dityrosine quantum yields are 0.12 (pH 4) and 0.16 (pH 10). Hence, in most cases the fluorescence quantum yields determined here are in rough agreement with previously reported values after they have been corrected to the same value for the quantum yield of tyrosine.

Dityrosine Anisotropy Decays

One of the clues to the identity of the species emitting at 400 nm in tyrosine samples was the long rotational correlation time. We measured a rotational correlation time of 130 to 180 ps over this wavelength region, with initial anisotropies of 0.29. In comparison, the tyrosine dipeptide (two tyrosine residues connected by a normal peptide linkage) has been reported by Lakowicz and Maliwal[41] to have a rotational diffusion time of 77 ps (in water). The rotational diffusion time of the dityrosine–borate complex is much longer than that of dityrosine measured at the same pH (pH 8). This result indicates that the molecule is larger or changes shape when bound to borate, a conclusion that is consistent with the borate complex structure proposed by Malencik and Anderson.[35]

The rotational correlation time is given in Stokes–Einstein–Debye (SED) theory by[42]

$$\tau_r = \frac{\eta V}{kT} F \tag{1}$$

where η is the solvent viscosity, V is the molecular volume, and F is the coupling factor that accounts for the shape and hydrodynamic boundary conditions ($F = 1$ for a sphere with "stick" boundary conditions). In order to scrutinize the rotational correlation times measured for dityrosine and dityrosine dipeptides in the context of SED equation, we calculated the molecular volumes of the energy minimized structures of dityrosine molecules in the molecular dynamics program CHARMM.[43] The dependence of the experimentally determined rotational times on volume is presented graphically in Fig. 11 and compared with the rotational correlation times of tyrosine species.[1]

A striking result in Fig. 11 is the strong dependence of the rotational time of the dityrosine species on molecular volume. The slope for the dityrosine species is larger by more than a factor of two than the SED prediction for a sphere with stick boundary conditions. Based on the estimated molecular volumes, the slope corresponds to a coupling factor $F = 2.0$ for the dityrosine and dityrosine dipeptides, compared to $F = 0.7$ for the tyrosine species. The large rotational times of the dityrosine species could reflect either a markedly nonspherical shape of dityrosine or an enhanced friction. In order for the large coupling factor F for dityrosine to be a consequence of shape, however, it would be necessary

to conclude that the shapes of the dityrosine species deviate from spherical to a much greater degree than do the shapes of the corresponding tyrosine molecules. We have estimated the shape factors of the dityrosine species by approximating their shape as an ellipsoid and found values of $F = 1.1$ to 1.3. Therefore, the large coupling factor for dityrosine cannot be attributed to shape.

A more likely possibility is that the dityrosine species experience an enhanced friction due to solvent interactions with the ionic changes of dityrosine, which at neutral pH exists as two linked zwitterions. These charges may engender stronger solute–solvent interactions compared to tyrosine species that consist of one zwitterionic pair. These solvent interactions may result from hydrogen-bonding interactions or from ionic or dielectric friction.[44] Dimerization of the dityrosine species can be excluded as an explanation of the long rotational correlation times because a concentration dependence was not observed. We note also that the rotational correlation time of dityrosine remains at least twice as long as tyrosine under high-pH conditions, where we have argued that dityrosine does not dimerize.

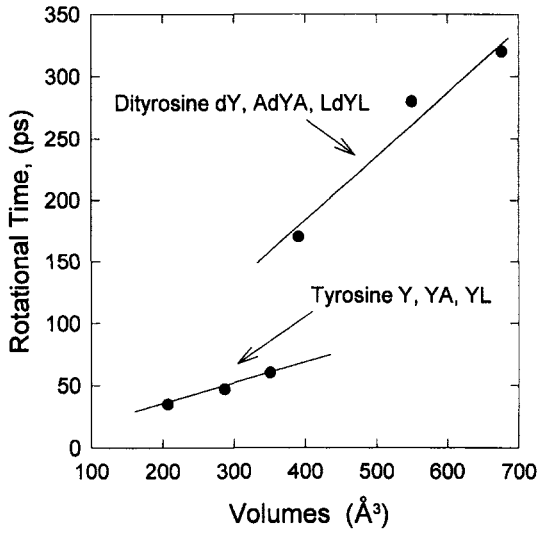

Fig. 11. Dependence of rotational correlation times on volume for dityrosine, alanine–dityrosine–alanine, and leucine–dityrosine–leucine. For comparison, the rotational correlation times of tyrosine, tyrosine–alanine, and tyrosine–leucine are shown (see Ref. 1). Volumes were estimated from the van der Waals volumes by molecular modeling (see text). The solid lines shows linear regression fit with slopes of 0.49 ps/Å³ for the dityrosine species and 0.17 ps/Å³ for the tyrosine species. The Stokes–Einstein–Debye prediction for a sphere and stick boundary condition is 0.25 ps/Å³.

CONCLUSIONS

Several features of dityrosine fluorescence recommend it as an intrinsic fluorescence probe. These include a relatively high fluorescence quantum yield, a distinct and relatively long fluorescence lifetime, and, for reorientational measurements, a reasonably high initial anisotropy ($r_0 = 0.25$ to 0.3). Importantly, dityrosine emission is red-shifted relative to protein fluorescence emanating from tyrosine or tryptophan.

We have found dityrosine emission, identified by red-shifted emission and longer rotational time, to be present in tyrosine samples. Under most conditions, two fluorescence lifetimes can be identified, one 250 to 800 ps and the other 2.5 to 4.5 ns. At a low pH (~2) a quenched species is formed. Over the pH range from pH 4 to 10, more subtle pH-dependent changes were observed with an apparent pK of ~7, corresponding to titration of a phenolic proton. We have suggested two models that are consistent with our observations. One involves emission from the anionic excited state, either produced directly by excitation of the anionic ground state or generated from the protonated species by rapid, unresolved excited-state proton transfer. The second model postulates distinct fluorescence from the protonated and anionic forms. Direct evidence in the form of a rise time (negative amplitude component) for an excited-state process was not observed.

The results reported here show that measurements of rotational correlation times can serve as an important diagnostic tool for identifying the nature of the rotating species. The rotational correlation time was important for identifying dityrosine fluorescence as a minor component in tyrosine samples. Rotational measurements also indicate a much larger solvent coupling factor than in tyrosine species. We attribute this to enhanced solute–solvent interactions resulting from the charges of the dityrosine species.

ACKNOWLEDGMENTS

We thank Dr. Stephen Fry and Dr. Geoffery Brady for their gift of a dityrosine sample. We are grateful to Prof. Graham Fleming and Dr. Gary Holtom for sharing their TCSPC fitting programs with us. J. F. H. was supported in part by an NSF Macro ROA grant. This work was supported by NSF EPSCoR Grant OSR-9255223 and by University of Kansas General Research allocation No. 3808.

REFERENCES

1. G. S. Harms, S. W. Pauls, J. F. Hedstrom, and C. K. Johnson (1997) *J. Fluoresc.* **7**, 273–282.
2. S. S. Lehrer and G. D. Fasman (1967) *Biochemistry* **6**, 757–767.
3. S. O. Andersen (1964) *Biochim. Biophys. Acta* **93**, 213–215.
4. C. A. Foerder and B. M. Shapiro (1977) *Proc. Natl. Acad. Sci. USA* **74**, 4214–4218.
5. P. Briza, G. Winkler, H. Kalchhauser, and M. Breitenbach (1986) *J. Biol. Chem.* **261**, 4288–4294.
6. P. Briza, A. Ellinger, G. Winkler, and M. Breitenbach (1990) *J. Biol. Chem.* **265**, 15118–15123.
7. N. Rabgaoui, A. Slaoui-Hasnaoui, and J. Torreilles (1993) *Free Rad. Biol. Med.* **14**, 519–529.
8. D. A. Malencik and S. R. Anderson (1994) *Biochemistry* **33**, 13363–13372.
9. S. F. Mahmoud and S. E. Bialkowski (1995) *Appl. Spectrosc.* **49**, 1677–1681.
10. D. A. Malencik and S. R. Anderson (1996) *Biochemistry* **35**, 4375–4386.
11. W. W. Westerfeld and C. Lowe (1942) *J. Biol. Chem.* **145**, 463–470.
12. A. J. Gross and I. W. Sizer (1959) *J. Biol. Chem.* **234**, 1611–1614.
13. G. S. Bayse, A. W. Michaels, and M. Morrison (1972) *Biochim. Biophys. Acta* **284**, 34–42.
14. Y. Ushijima, M. Nakano, and T. Goto (1984) *Biochem. Biophys. Res. Commun.* **125**, 916–918.
15. R. Amadò, R. Aeschbach, and H. Neukom (1984) *Methods Enzymol.* **107**, 377–388.
16. K. Kikugawa, T. Kato, and A. Hayasaka (1991) *Lipids* **26**, 922–929.
17. J. W. Heinecke, W. Li, H. L. Daehnke, and J. A. Goldstein (1993) *J. Biol. Chem.* **268**, 4069–4077.
18. T. G. Huggins, M. C. Wells-Knecht, N. A. Detorie, J. W. Baynes, and S. R. Thorpe (1993) *J. Biol. Chem.* **268**, 12341–122347.
19. T. T. Tominaga and M. Tabak (1995) *Anal. Chim. Acta* **315**, 217.
20. L. A. Marquez and H. B. Dunford (1995) *J. Biol. Chem.***270**, 30434–30440.
21. D. A. Malencik, J. F. Sprouse, C. A. Swanson, and S. R. Anderson (1996) *Anal. Biochem.* **242**, 202–213.
22. K. Kikugawa, T. Kato, and Y. Okamoto (1994) *Free Rad. Biol. Med.* **16**, 373–382.
23. J. P. Eiserich, A. v. d. Vliet, G. J. Handelman, B. Halliwell, and C. E. Cross (1995) *Am. J. Clin. Nutr.* **62** (Suppl.), 1490S–1500S.
24. S. Garcia-Castineiras, J. Dillon, and A. Spector (1978) *Science* **199**, 897–899.
25. K. Kikugawa, T. Kato, M. Beppu, and A. Hayasaka (1991) *Biochim. Biophys. Acta* **1096**, 108–114.
26. V. J. Malanik and M. Ledvina (1979) *J. Chromatogr.* **170**, 254.
27. K. Zaitsu, S. Eto, and Y. Ohkura (1981) *J. Chromatogr.* **206**, 621–624.
28. S. F. Mahmoud and S. E. Bialkowski (1995) *Appl. Spectrosc.* **49**, 1669–1676.
29. E. W. Small and S. R. Anderson (1988) *Biochemistry* **27**, 419–428.
30. A. J. Kungl, G. Landl, A. J. W. G. Visser, M. Breitenbach, and H. F. Kauffmann (1992) *J. Fluoresc.* **2**, 63–74.
31. A. J. Kungl, A. J. W. G. Visser, H. F. Kauffmann, and M. Breitenbach (1994) *Biophys. J.* **67**, 309–317.
32. L. J. Libertini and E. W. Small (1985) *Biophys. J.* **47**, 765–772.
33. A. J. Kungl, M. Breitenbach, and H. F. Kauffmann (1994) *Biochim. Biophys. Acta* **1201**, 345–352.
34. S. O. Andersen (1963) *Biochim. Biophys. Acta* **69**, 249–262.
35. D. A. Malencik and S. R. Anderson (1991) *Biochem. Biophys. Res. Commun.* **178**, 60–67.
36. D. V. O'Connor and D. Phillips. (1984) *Time-Correlated Single Photon Counting*, Academic Press, London, Orlando, FL.
37. J. B. A. Ross, W. R. Laws, A. Buku, J. C. Sutherland, and H. R. Wyssbrod (1986) *Biochemistry* **25**, 608–612.
38. S. Sakura and D. Fujimoto (1984) *Photochem. Photobiol.* **40**, 731–734.
39. F. W. J. Teale and G. Weber (1957) *Biochem. J.* **65**, 476–482.
40. R. F. Chen (1967) *Anal. Lett.* **1**, 35–42.
41. J. R. Lakowicz and B. P. Maliwal (1983) *J. Biol. Chem.* **258**, 4794–4801.
42. C. R. Cantor and P. R. Schimmel (1980) *Biophysical Chemistry*, W. H. Freeman, New York, Vol. II.
43. B. R. Brooks, R. Bruccoleri, B. Olafson, D. States, S. Swaminathan, and M. Karplus (1983) *J. Comp. Chem.* **4**, 187–217.
44. N. Balabai and D. H. Waldeck (1997) *J. Phys. Chem. B* **101**, 2339–2347.
45. A. J. Kungl (1992) *Biophys. Chem.* **45**, 41–50.